Rhodopsin–Phospholipid Complexes in Apolar Environments: Photochemical Characterization†

A. Darszon,* R. J. Strasser,‡ and M. Montal

ABSTRACT: Rhodopsin was transferred, as a protein–lipid complex, in its unbleached state from retinal rod outer segments (ROS) into organic solvents by a novel technique not involving detergents. The optical absorbance properties of rhodopsin were examined in (a) the organic solvent and in (b) the protein–lipid complex hydrated after solvent evaporation. (a) In hexane and in ether the difference spectra between dark and irradiated samples show λ_{max} at 499 ± 1 nm and isosbestic points around 415 ± 4 nm. Bleached rhodopsin in hexane, but not in ether, when supplemented with 9-*cis*-retinal, regenerated isorhodopsin with a yield of better than 90%. (b) Rhodopsin from ether extracts was deposited in a filter paper disk (Whatman), the solvent evaporated, and then the complex hydrated. At room temperature rhodopsin showed absorption spectra in the dark and after bleaching similar to those recorded in ROS membranes; on addition of 11-*cis*-retinal to the filter paper, regeneration of rhodopsin to ~95% was obtained. When rhodopsin was bleached at −196 °C and spectra were recorded as a function of temperature (from −196 to 20 °C), the expected displacements of λ_{max} due to the production of the intermediates (batho, lumi, meta I, meta II, and meta III) were observed. The photochemical functionality of this preparation was also evaluated by measuring the kinetics of the metarhodopsin I to metarhodopsin II transition simultaneously at 478 and 380 nm, respectively. The temperature and pH dependencies of this reaction were comparable to the values reported for rhodopsin in ROS membranes. The kinetics of this photochemical conversion were also recorded in hexane and ether. The results indicate that rhodopsin derived from hexane and ether extracts conserves the basic spectral features it displays in native retinal ROS disk membranes and, therefore, constitutes an active starting point for reconstitution studies in planar bilayers and other model membranes.

Photon capture by rhodopsin, the visual pigment of the retinal photoreceptor cells, triggers the excitation of the visual system [Hecht et al., 1942; Wald, 1968; for a review, see Ebrey & Honig (1975)]. Upon exposure to light, rhodopsin bleaches through a series of intermediates (Yoshizawa, 1972; Ostroy, 1977). Along this sequence of events the ionic permeability of the plasma membrane is altered and thus the arrival of a photon is translated into an electrical response. Although much is known about retinal photoreceptor physiology, the mechanism that links the photochemical changes of rhodopsin to the neural response remains largely unsolved (Hagins & Yoshikami, 1977; Ostroy, 1977).

We have approached this problem by incorporating rhodopsin in model membranes. To achieve this, we have developed and characterized techniques that allow the extraction of unbleached rhodopsin–lipid complexes (RLC)[1] into organic solvents (Montal & Korenbrot, 1973; Darszon et al., 1977, 1978a). The RLCs in organic solvents are the building blocks of the model membranes; they spread into monolayers at air–water interfaces which are subsequently used to form planar bilayers (Montal, 1974; Montal et al., 1977; Trissl et al., 1977). Alternatively, black films are readily formed by spreading the extracts in the organic phase (Montal, 1974; Chien & Mueller, 1976). Bilayer vesicles spontaneously form from the complex after solvent evaporation and subsequent hydration in salt media (Montal, 1974) or by sonication of the complex in the solvent with aqueous buffer followed by solvent evaporation under reduced pressure (Darszon et al., 1979).

A successful functional reconstitution in model membranes is necessarily evaluated by the retrieval of the biological activity of the system. With rhodopsin, however, the model system is being used in an effort to establish the function (Montal et al., 1977; O'Brien et al., 1977; Hubbell et al., 1977). Accordingly, it is necessary to compare other known characteristics of the protein in its natural environment with those observed in model systems. Our purpose in this paper is to establish that irradiation of the dark rhodopsin–lipid complexes extracted with organic solvents generates the same photoproducts as those found in native ROS membranes.

The ultimate test for the presence of spectrally native rhodopsin in the reconstituted planar lipid bilayer would be to record the absorption spectra of the bilayer itself. At present, this is technically difficult. To circumvent this problem, we developed a system to study the material from which the bilayer is formed under the conditions in which the bilayer is studied. It consists of a filter paper disk used as a rigid, porous matrix upon which the ether extract is layered and then hydrated as to simulate the process of spreading the extract at air–water interfaces.

We also report the kinetics and pH dependence of the metarhodopsin I to metarhodopsin II transition. This photochemical conversion precedes the electrical photoresponse of rhodopsin-containing cells and is considered, therefore, to be of major functional importance in the transduction process [for reviews, see Hagins (1972) and Ostroy (1977)]. The main conclusions advanced are that rhodopsin does not undergo major photochemical changes when it is extracted into apolar environments as described and that the rhodopsin–lipid complexes constitute an active starting point for reconstitution in planar bilayers and other model membranes.

Preliminary accounts of this research were presented else-

† From the Departments of Biology (R.J.S. and M.M.) and Physics (A.D. and M.M.), University of California, San Diego, La Jolla, California 92093. *Received February 23, 1979.* This work was supported by National Eye Institute Grant EY-02084.

‡ Present address: Institute de Physiologie Vegetale, 1211 Geneve, Switzerland.

[1] Abbreviations used: ROS, rod outer segments; DDAO, dodecyldimethylamine oxide; RLC, rhodopsin–lipid complex; ΔA_{500}, absorbance difference between dark and bleached samples at 500 nm; A, absorbance; K, rate constant; λ_{max}, wavelength of maximum absorbance.

0006-2960/79/0418-5205$01.00/0

where (Darszon et al., 1978b; Strasser et al., 1978; Montal et al., 1978).

Materials and Methods

The following materials were obtained from the indicated sources: dark-adapted bovine retinas (Hormel Co., Austin, MN); L-α-lecithin from soybeans and 9-*cis*-retinal (Sigma Chemical Co., St. Louis, MO); 11-*cis*-retinal (kindly supplied by Dr. W. E. Scott, Hoffmann-La Roche, Nutley, NJ); nucleopore filters (Nucleopore Co., Pleasanton, CA); Whatman no. 1 filter paper (W & R Balston, Ltd., England); dodecyldimethylamine oxide (DDAO) (Onyx Chemical Co., Hoboken, NJ).

All the procedures were performed under dim red light at 4 °C unless otherwise stated. Rod outer segments (ROS) from dark-adapted bovine retinas were isolated by sucrose flotation and purified in a discontinuous sucrose gradient (McConnell, 1965; Papermaster & Dreyer, 1974). The rhodopsin concentration in the purified ROS was determined by solubilizing an aliquot in 3% (w/v) dodecyldimethylamine oxide (DDAO) (Ebrey, 1971) and 60 mM phosphate, pH 7.0, and measuring the difference in the absorbance at 500 nm (ΔA_{500}) between dark and bleached samples, assuming an extinction coefficient of 42 000 M^{-1} cm^{-1} (Wald & Brown, 1953) and a molecular weight of 37 000 [cf. Ebrey & Honig (1975)]. The ratio of absorbance at 280 and 500 nm, A_{280}/A_{500}, ranged from 2.6 to 3.4.

Direct Transfer of Rhodopsin from ROS Membranes into Organic Solvents. The following protocol was used to directly transfer rhodopsin from ROS membranes preferentially into ether (Darszon et al., 1978a). ROS membrane aliquots in 10 mM imidazole–HCl buffer, pH 7.0, containing ~0.75 mg of rhodopsin were centrifuged at 27000*g* for 20 min, and the supernatant was removed. The ROS pellet was resuspended in 1 mL of hexane containing 15 mg of partially purified soybean phospholipids (Kagawa & Racker, 1971). The resulting ROS dispersion in hexane was immediately sonicated for 5 min in a water bath sonicator. Thereafter, 0.1 mL of 0.1 M $CaCl_2$ was added and the mixture stirred on a vortex mixer for 20 s. The preparation was centrifuged in a clinical centrifuge (4 min at maximum speed) and the hexane phase removed. The remaining ROS-containing aqueous emulsion was subsequently extracted with 1 mL of pure ether (diethyl ether) on a vortex mixer for 3 min. The suspension was centrifuged (1 min at 4/7 maximum speed) and the organic phase removed. The ether extract had an average ΔA_{500} of ~0.3 in a 1-cm light path cuvette, a phospholipid/protein ratio of ~300, and a rhodopsin/total protein ratio of 0.8 (Darszon et al., 1978a). For preferential transfer of rhodopsin from ROS membranes into hexane, the protocol was modified as follows: only one extraction into hexane was performed, the ROS dispersion in hexane was sonicated for 7 min, 0.1 mL of 1 M $CaCl_2$ was added after sonication, and the mixture was vortexed for 2 min. The hexane extract had an average ΔA_{500} of ~0.26 and a phospholipid/protein ratio of ~2000 (Darszon et al., 1978a).

Spectroscopic Measurements. Spectra were recorded by using a multifiber optic system (Strasser, 1973) connected to a modified Cary 14 spectrophotometer on line with a PDP-8 minicomputer (Digital Equipment Corp., Maynard, MA), as described previously (Butler & Hopkins, 1970). The spectral analysis of rhodopsin in hexane and in ether was carried out in 1-cm path length spectroscopic cuvettes sealed with Teflon stoppers to avoid evaporation. The absolute spectra were generated by subtracting the base line recorded with the corresponding solvent in the absence of sample.

The rhodopsin–lipid complex left after evaporation was studied as follows. Disks of 1 cm in diameter were cut from Whatman no. 1 filter paper. A series of disks was arrayed over a microscope slide in the 4 °C dark room, and aliquots (100–300 μL) of the ether extract were layered on them. This was accomplished by the sequential application of 50 μL of the RLC extract per disk, allowing sufficient time for solvent evaporation. Thereafter, the disks were hydrated and buffered with 1:1 glycerol–60 mM phosphate buffer, pH 7.0 (80 μL), unless otherwise stated. The filter paper disks were then kept for spectral analysis (usually performed within a few hours) in a petri dish containing a filter paper slightly humidified with the glycerol–phosphate buffer mixture, inside a light-tight metal box at 4 °C. The RLC in the disk prepared as described, when wet, was stable in terms of its spectroscopic behavior for at least 5 days (no tests were performed after longer periods).

The spectra of the RLC in the disks were taken in a circular metal holder where the sample was sandwiched between two circular glasses of the same diameter and sealed from the exterior by a metal cylinder that pressed the two glasses together through an O-ring. The metal cylinder also served as a guide to hold the light pipe in the center of the sample. Low-temperature spectroscopy was performed with a similar arrangement. The cylinder, however, was a stainless steel block of 500 g to increase the heat capacity. The bottom part of the cuvette had an opening leading to the sample where a copper–constantan thermocouple was introduced. The thermocouple was connected to an x–y recorder to monitor the exact temperature of the filter paper at all times during the experiment. A Teflon container surrounding the cuvette was filled with liquid nitrogen, cooling the sample block to −196 °C. Once the temperature settled at −196 °C, the dark spectrum was recorded and the sample was illuminated with 440-nm light for the indicated periods of time, using a tungsten lamp and a Balzers interference filter, giving 200 $\mu W/cm^2$ at 440 nm. Spectra were measured and stored in core memory after each period of illumination. After evaporation of the liquid nitrogen, the metal block began to warm up, increasing the sample temperature slowly and smoothly. During this process both the spectrum and the temperature corresponding to each measurement were assayed simultaneously and the spectra stored in the computer for further analysis. The base line was recorded and stored by measuring, under the same conditions, the spectrum of a humid filter paper disk without the RLC residue. The absolute spectra were generated by subtracting this base line.

All spectra were measured from 400 to 700 nm and stored as 750 digital values in the minicomputer. The data were then transferred to a microcomputer system (ARETE 100, San Diego, CA) where they were processed for the following calculations: the absorbance difference between sample and reference; the spectral difference of the sample in two different conditions; the first derivative of the spectra. The records shown were plotted directly by the microcomputer system.

Kinetic Measurements. The RLCs in the wet filter paper were sandwiched between two thin glass disks held together and sealed within a steel cuvette. The cuvette was then immersed in a Dewar containing ice water or water at the needed temperature. Figure 1 shows a diagram of the setup; a multibranched fiber optic system (Strasser, 1973; Strasser & Butler, 1976) was mounted at the top and bottom of the sample. This arrangement allowed two measuring beams, MB_1, 478 ± 2 nm (100-W tungsten lamp and Bausch and Lomb monochromator set at 478 nm), and MB_2, 380 ± 2 nm (150-W

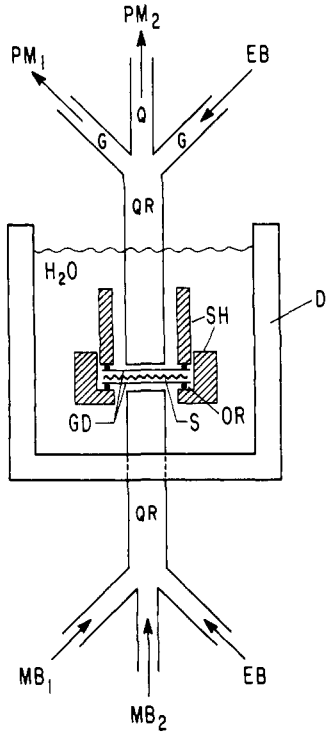

FIGURE 1: Experimental setup for excitation and two simultaneous absorption measurements of a sample: (S) sample; (SH) sample holder; (GD) glass disks; (OR) O-ring; (D) Dewar; (QR) quartz rod (it also acts as a light-mixing rod to provide homogeneous illumination to the sample); (Q) light pipe of quartz fibers; (G) light pipe of glass fibers; (MB) measuring beams; (EB) exciting beam; (PM) photomultipliers.

tungsten lamp, Bausch and Lomb monochromator set at 380 nm, and a Corning CS 5970 glass filter), to cross from the lower light pipes through the sample into the upper light pipes and from there to the phototubes PM_1 (Hamamatsu S20 type plus Corning CS 5562 glass filter and Balzer 478-nm interference filter) and PM_2 (Hamamatsu S20 type plus Balzer 380-nm interference filter). The third light pipe on both sides of the sample was used for the excitation beam (EB), 550 ± 30 nm (xenon flash <1 ms, 3×10^{-5} J/cm^2 intensity, Honeywell Pressmaster 800 and two Corning CS 3384 glass filters).

The experimental setup was connected, on line, to the microcomputer data acquisition system ARETE 100 (Arete Instruments, San Diego, CA). The signals generated by two photomultipliers were simultaneously digitized in 2000 words of 12-bit resolution per signal and stored in the core memory of the microcomputer unit. All the curves presented in the figures show the experimental data and their mathematical transformations calculated and plotted by the computer. Before being plotted, the curves were convoluted by continuously averaging eight digitized data points.

Rhodopsin Regeneration. Rhodopsin regeneration was assayed in the filter paper disk as follows. The sample was prepared as described, but a fivefold excess of 11-*cis*-retinal (molar basis with respect to rhodopsin) dissolved in hexane (50 μL) was added in the dark to the ether extract before depositing it in the disk. The dark spectrum was then recorded, the sample bleached with white light, and its spectrum determined. Thereafter, the disk was kept in the dark and spectra were measured at the indicated time.

Regeneration of rhodopsin in hexane was assayed as follows. RLCs were extracted into hexane (as described), and the dark and totally bleached spectra were recorded. Subsequently, an aliquot of concentrated 9-*cis*-retinal solution in hexane was added in the dark at fivefold excess with respect to rhodopsin (molar basis). The sample was incubated in the dark, and spectra were recorded at the indicated intervals.

Results and Discussion

Absorbance Characteristics of the Rhodopsin–Lipid Complex at Room Temperature. The absolute and difference absorbance spectra of RLC in hexane and ether and in the filter paper disk after ether evaporation are illustrated in Figure 2. The difference spectra between dark (1) and irradiated (2) samples obtained 2 to 3 min after bleaching show absorbance maxima (λ_{max}) at 502, 503, and 504 nm, respectively, and isosbestic points at 418, 422, and 423 nm, respectively.

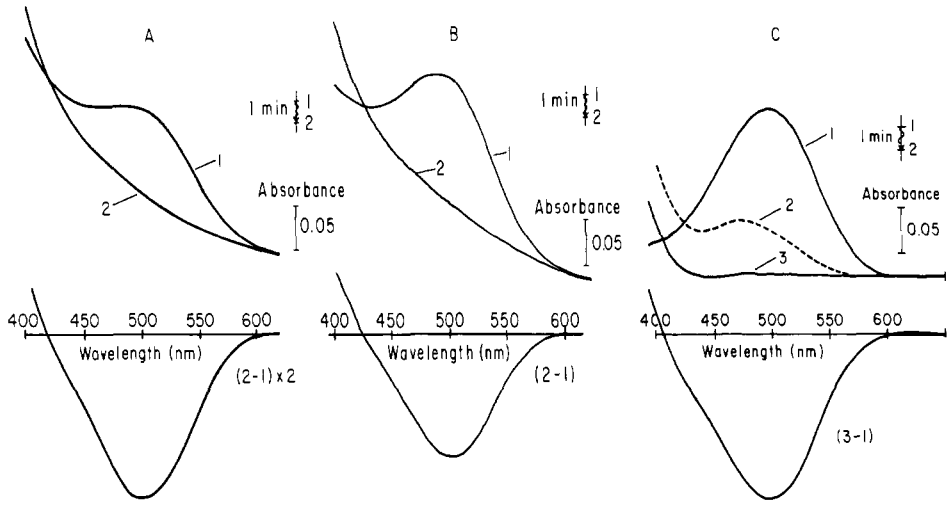

FIGURE 2: Absolute and difference spectra of rhodopsin–lipid complexes in hexane (A), in ether (B), and in a filter paper disk (C). The wavy line in the upper right quadrant of each spectra indicates the length of the illumination period. Spectra of the RLC in hexane and ether were recorded with 1-cm path length cuvettes. The extracts were prepared as described under Materials and Methods. The RLC in hexane was diluted threefold and the ether extract twofold. Difference spectra were obtained by subtracting the dark spectrum (1) from the bleached one (2). The filter paper was prepared by layering 200 μL of an ether extract. After being bleached (curve 2), the sample was incubated for 30 min with 0.1 M hydroxylamine and spectrum 3 recorded. The difference spectrum was obtained by subtracting the dark spectrum (1) from the bleached one (3) obtained in the presence of hydroxylamine. Filter papers prepared as described but hydrated with buffer supplemented with 0.1 M hydroxylamine showed spectra in the dark and after bleaching comparable to those displayed in (1) and (3). All spectra were recorded at room temperature and bleached with white light.

The values for λ_{max} and isosbestic points obtained are red-shifted with respect to those displayed in the native membrane, i.e., 498 and 418 nm. The red shift of the difference spectra could be attributed to the contribution of a mixture of the long-lived photoproducts metarhodopsin III (λ_{max} 465 nm) and *N*-retinylideneopsin (λ_{max} 440 nm) (Ostroy, 1977); the possibility was tested as follows. For the organic extracts, difference spectra were recorded 1 h after bleaching. The spectra showed λ_{max} at 499 ± 1 nm and an isosbestic point at 414 ± 1 nm. Furthermore, extractions performed with membranes deliberately pelleted and extracted in the presence of hydroxylamine (0.1 M) displayed in hexane a λ_{max} at 499 ± 1 and an isosbestic point at 406 ± 1 nm. Similarly, in ether the λ_{max} was at 499 ± 1 nm and the isosbestic point was at 400 ± 1 nm. The fact that rhodopsin bleaches in the organic extracts implies the presence and accessibility of H_2O (see Figure 6) in the solvent and explains the effect of the extracted hydroxylamine in the apolar media. For RLC in the filter paper, samples were incubated for 30 min with 0.1 M hydroxylamine; this allowed complete bleaching (line 3 in Figure 2C), eliminating the appearance of photoproducts absorbing at ~440 nm (see Figure 3B). Therefore, in this condition the difference spectrum 3-1 was not contaminated with slow intermediates and showed λ_{max} at 499 ± 1 nm and an isosbestic point at 407 ± 1 nm.

The hexane and ether extracts are turbid and probably exist emulsified (Darszon et al., 1978a). The scattering of hexane and ether extracts containing equivalent rhodopsin concentrations was measured at 650 nm, where neither the protein nor the lipid absorbs. These values are 0.08 ± 0.02 (n = 4) for hexane and 0.26 ± 0.05 (n = 7) for ether, suggesting that their particle size is different. Indeed, it was found that on passing the extracts through nucleopore filters of defined pore sizes the hexane extract passed through a 0.4-μm pore whereas the complex in ether was retained.

Rhodopsin Regeneration. The spectral characteristics of the RLC in the organic phase and in the filter paper presented so far resemble those displayed by rhodopsin in ROS disk membranes but do not provide information concerning the native state of the final product, opsin. A very sensitive criterion of the native state of rhodopsin is the ability of opsin to combine with 11-*cis*- (or 9-*cis*-) retinal to regenerate rhodopsin (or isorhodopsin) (Hubbard & Wald, 1952). It is known that, in some circumstances, rhodopsin may preserve its spectral characteristics but lose its regeneration capacity; that is the case for rhodopsin solubilized in some detergents (Heller, 1968; Johnson & Williams, 1970; Shichi, 1971) or in old disk membranes.

Figure 3A shows that opsin in hexane combines with 9-*cis*-retinal to regenerate isorhodopsin to ~45% in 30 min and that full regeneration (90 ± 8%, n = 3) is achieved in 2.5 h (not shown). The difference spectra 2-1, 3-1, and 4-1 result from subtracting the totally bleached spectrum without 9-*cis*-retinal (1) from the spectra measured after the addition of retinal and the indicated incubation periods in the dark. The blue shift of peak 6-4 can be accounted for by the contribution of the simultaneous decay of metarhodopsin III to opsin from the previous bleaching. As shown in Figure 3B, the regeneration of rhodopsin in the filter paper amounted to 65% within 45 min and to 91 ± 7% (n = 4) within an hour (not shown). Notice that the difference spectra contain contributions from rhodopsin formed from 11-*cis*-retinal and opsin as well as from metarhodopsin III. A noticeable point in this figure is the fact that two products are appearing with different kinetics; the fastest one, displaying a λ_{max} at 440 nm in difference spectra

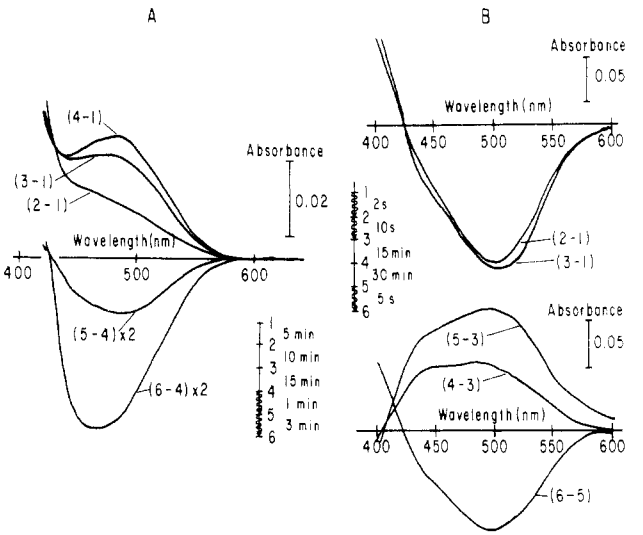

FIGURE 3: Rhodopsin regeneration in hexane (A) and in the filter paper disk (B). The experimental protocol is indicated in the inset: wavy and straight lines respectively indicate light and dark periods of assigned duration. (A) Rhodopsin extracted into hexane was completely bleached, and the spectra were recorded. Thereafter, an aliquot of 9-*cis*-retinal in hexane was added to obtain a fivefold excess with respect to rhodopsin (molar basis). The difference spectra 2-1, 3-1, and 4-1 were obtained by subtracting the totally bleached spectrum without 9-*cis*-retinal (1) from the spectra measured after the addition of retinal and the indicated incubation periods in the dark. Curves 5-4 and 6-4 illustrate the bleaching of the regenerated isorhodopsin (see text). (B) The ether extract was supplemented in the dark with a concentrated solution of 11-*cis*-retinal in hexane at a fivefold excess with respect to rhodopsin (molar basis); the disk was then prepared by layering the extract (300 μL) as described. Curves 2-1 and 3-1 represent the difference spectra of the bleached minus dark conditions. A second bleaching (10 s) was performed to assure total bleaching. Both regenerations were performed at room temperature.

4-3 and 5-3, appears within the first 10 min after the phototransformation of rhodopsin, provided the temperature is higher than 0 °C. This could be attributed to the formation of long-lived photoproducts (e.g., metarhodopsin III and *N*-retinylideneopsin). The difference spectrum 6-5 results from bleaching the regenerated rhodopsin and displays a λ_{max} at 500 nm. Similar results were reported by Paulsen et al. (1975) in ROS derived from bullfrog retinas. Our data indicate that rhodopsin in RLC extracts exhibits a regeneration capability comparable in magnitude to that of rhodopsin in cell membranes.

The kinetics of rhodopsin regeneration vary according to the experimental protocol. In ROS membranes, when regeneration proceeds immediately after bleaching, the time course of the reaction is slower than when regeneration is initiated after the decay of the photoproducts. This suggests that the presence of the long-lived intermediates limits the regeneration rate (Paulsen et al., 1975). These are the experimental conditions prevalent during rhodopsin regeneration in hexane and in the filter disks, and, therefore, the similarity of the reaction time course could be explained in the same way. Alternative explanations invoking changes in the environment of opsin cannot, at present, be ruled out particularly in light of the fact that digitonin, considered by many as a mild detergent, inhibits the regeneration rate (Wald & Brown, 1956; Matsumoto et al., 1978).

Photointermediates of the Ether-Extracted Rhodopsin in the Filter Paper. A more detailed analysis of the photochemical functionality of RLC in the filter paper involves the determination of the rhodopsin bleaching sequence by low-temperature spectroscopy (Yoshizawa & Wald, 1963, 1966;

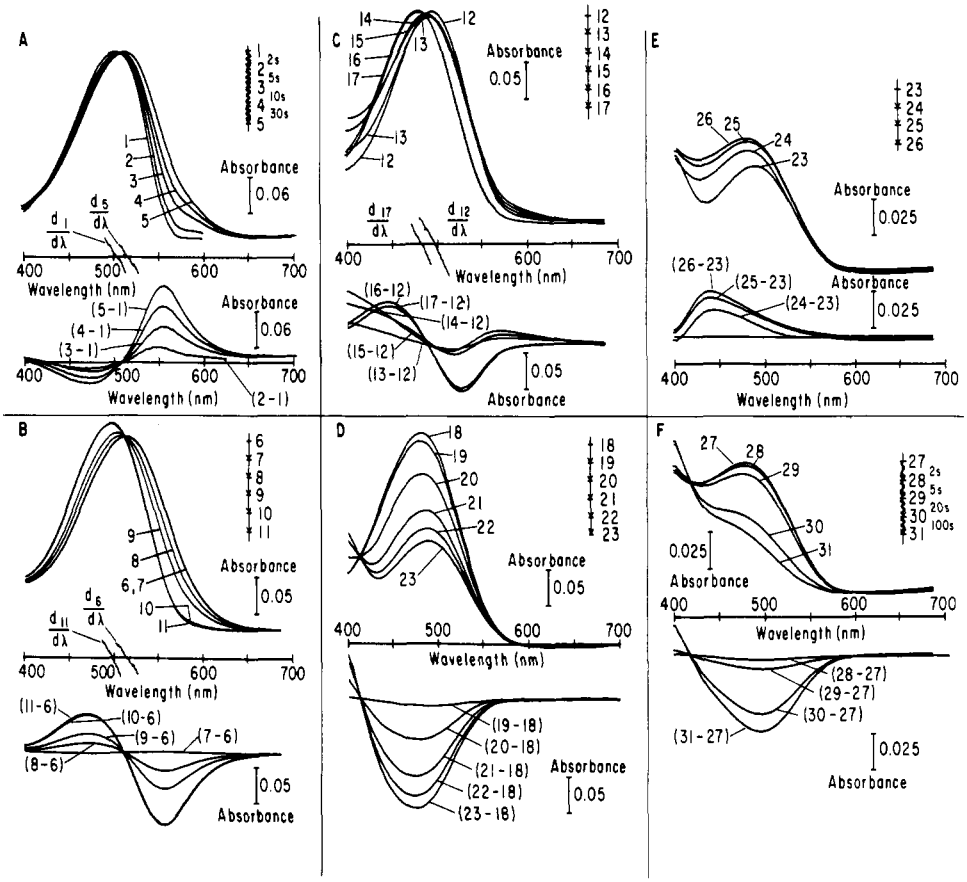

FIGURE 4: Low-temperature study of the bleaching sequence of rhodopsin in the filter paper disk. The filter paper disk was prepared as described under Materials and Methods by layering 300 μL of an ether extract. The experimental protocol is shown in the inset: wavy lines indicate illumination periods of the assigned duration; straight lines illustrate the warming process in the dark; the arrow points indicate the direction of increasing temperature. Each number corresponds to an absolute spectrum, and the difference spectra are identified with the subtraction of the absolute spectra from which they result. The lines which cross the wavelength axis represent the first derivative ($d_n/d\lambda$) of the spectrum indicated with the corresponding number. (A) Photoconversion of rhodopsin measured at −196 °C. RLCs in the filter paper were cooled with liquid nitrogen in the dark, and the spectra were recorded and then bleached with 440-nm light for the indicated time periods, thus producing a mixture of rhodopsin, isorhodopsin, and bathorhodopsin. (B) Thermal conversion of bathorhodopsin to lumirhodopsin. The liquid nitrogen was allowed to evaporate and the metal cell holder slowly warmed up. Curves 6 and 7 were recorded at −150 and −140 °C, respectively, and represent the mixture of rhodopsin, isorhodopsin, and bathorhodopsin which was stable up to this temperature. Curves 8–11 are the spectra of the products formed by warming in the dark to −135, −128, −113, and −82 °C, respectively. (C) Thermal conversion of lumirhodopsin to metarhodopsin I. Curves 12–17 were recorded at −70, −66, −63, −45, and −30 °C, respectively. (D) Thermal conversion of metarhodopsin I to metarhodopsin II. Curves 18–23 were recorded at −14, −10, −5, −2, −1, and 0 °C, respectively. (E) Thermal conversion of metarhodopsin II to metarhodopsin III. Curves 23–26 were recorded at 0, 10, 13, and 20 °C, respectively. (F) Bleaching of the remaining fraction of rhodopsin and isorhodopsin at room temperature. The illumination periods are as indicated.

Yoshizawa, 1972). The photoproducts of rhodopsin in disk membranes, retinas, and digitonin solutions have been established by this technique (Kawamura et al., 1977) and provide a convenient frame of reference.

The results of this study are illustrated in Figure 4. When the wet filter paper disk in the glycerol–phosphate buffer mixture was cooled to −196 °C, the λ_{max} of rhodopsin shifted from 503 to 507 nm with a corresponding 8% increase in absorption. In addition, the chromophore band sharpened at this temperature as expected. Irradiation of the sample at −196 °C with monochromatic light (440 nm) shifted the spectrum to longer wavelengths with a new maximum at 515 nm (see Figure 4A, curve 5). The difference spectra show an isosbestic point at ~510 nm with a λ_{max} at 556 nm; this indicates the formation of bathorhodopsin. The lines which cross the wavelength axis represent the first derivative of the indicated spectrum and correspond to the respective λ_{max}. The final spectrum is stable at −196 °C and represents a mixture of rhodopsin, isorhodopsin, and bathorhodopsin.

Thereafter, the liquid nitrogen was allowed to evaporate and as the sample slowly warmed up, spectra and temperature were recorded continuously without further illumination. Since the temperature was rising steadily, the difference spectra reported, with the exception of the first transition, were obtained by subtracting two spectra at slightly different temperatures. This may introduce small changes in the sharpness and exact position of the peaks and must be considered when comparing the absolute spectra with the spectral intermediates reported in the literature.

The first spectral shift in the thermal conversion of bathorhodopsin started at ~−140 °C. The hypsochromic displacement showed a λ_{max} at 498 nm (Figure 4B). The difference spectra for this transition, which ended at ~−115 °C, show the disappearance of the peak at 556 nm and the appearance of an intermediate absorbing at shorter wavelengths. These changes correlate with the transition of bathorhodopsin to lumirhodopsin. Immediately after, at ~−70 °C, the following displacement toward the blue began: within the temperature region of −70 to −30 °C the glycerol–water glass becomes opalescent (Yoshizawa & Wald, 1966), and concurrent with the shift of λ_{max} the absorbance increased and then decreased. The λ_{max} shifts from 498 nm first to 486 nm and then to 480 nm, reflecting the transition from lumirhodopsin to metarhodopsin I (Figure 4C). The lumirhodopsin to metarhodopsin

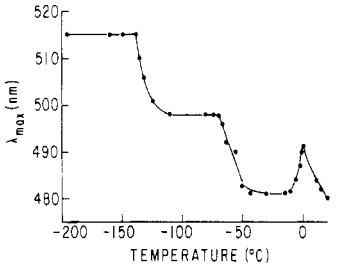

FIGURE 5: Profile of the λ_{max} displacements of the absolute spectra in the bleaching of rhodopsin as a function of temperature. RLCs in the filter paper (300 μL of ether extract) were cooled to liquid nitrogen temperature and irradiated at 440 nm, producing a mixture of rhodopsin, isorhodopsin, and bathorhodopsin. Then the preparation was allowed to warm, and the temperature and spectra were continuously recorded without further illumination.

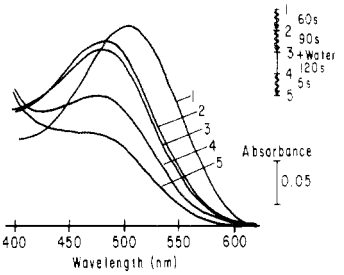

FIGURE 6: Stability of metarhodopsin I at room temperature in a dry filter paper. The bleaching sequence of rhodopsin in a dry filter paper (no addition of buffer after layering the RLC in ether) was performed as in Figure 4. The experimental protocol appears in the inset: wavy lines indicate the duration of irradiation (440 nm); the straight line illustrates a dark period. Curve 1 was recorded in the dark at −196 °C; thereafter, the sample was illuminated with 440-nm light and the temperature allowed to increase. Curve 2 was recorded at room temperature, showing that the bleaching sequence has been arrested at the metarhodopsin I stage. The sample was further irradiated at this temperature (curve 3), displaying almost no change. At this point, water was introduced in the sample holder, wetting the filter paper and allowing the metarhodopsin I to metarhodopsin II transition to occur (curve 4). Finally, the wet sample was again illuminated, bleaching a fraction of the remaining rhodopsin (curve 5).

conversion ends at around −13 °C. At this point, as the sample warms from −13 to 2 °C, the 480-nm band decreases with a simultaneous increase of absorption at lower wavelength (<416 nm). This step can be identified as the metarhodopsin I to metarhodopsin II transition and is presented in Figure 4D. The absolute spectra show that as metarhodopsin I decreases the λ_{max} shifts toward the red. This is to be expected since, as we mentioned before, bleaching at −196 °C left a fraction of unbleached rhodopsin and isorhodopsin (30%); as they become predominant in the visible region, they determine the position of λ_{max}. The difference spectra of this transition exhibit a λ_{max} at 478 nm (Yoshizawa, 1972) and an isosbestic point at 416 nm. Continued warming (2–20 °C) shifted the spectra toward the blue with an increase of absorbance at around 440 nm (Figure 4E). This is clearly seen in the difference spectra and is consistent with the initial conversion of metarhodopsin II to metarhodopsin III.

When no further change was observed at room temperature and most of the intermediates in the thermal decay of bathorhodopsin had gone to the final products, *trans*-retinal and opsin, the sample was irradiated (440 nm light), thus bleaching the residual rhodopsin and isorhodopsin (Figure 4F). The difference spectra of this final phototransformation show a λ_{max} at 498 nm with an isosbestic point at 418 nm. Both λ_{max} and the isosbestic point in these spectra are at a slightly shorter wavelength than those presented in Figure 2C; this is consistent with the presence of some isorhodopsin in the sample. A profile of the λ_{max} displacements of the absolute spectra as a function of temperature is illustrated in Figure 5. The overall behavior of λ_{max} with respect to temperature is very similar, considering experimental differences, to that reported for rhodopsin in the frog retina (Tokunaga et al., 1976). The low-temperature study was repeated 4 times, yielding similar results.

The low-temperature study performed on dry samples (RLC in the filter paper disk without the glycerol–phosphate buffer mixture) yielded, up to −13 °C, similar results to those obtained for the wet paper filter. At this stage the lumirhodopsin to metarhodopsin I transition ends. It is known that metarhodopsin I can be formed in the dry state (Wald et al., 1950). In contrast, the conversion of metarhodopsin I to metarhodopsin II depends critically on the nature and pH of the solvent (Ostroy, 1977). At −13 °C the thermal decay of bleached rhodopsin in the dry sample stopped almost completely, remaining at the metarhodopsin I stage up to room temperature. Furthermore, on reaching room temperature the sample was illuminated again with a strong white light, causing only a discrete bleaching (Figure 6, curve 3). Thereafter, the sample was slowly hydrated and the conversion from metarhodopsin I to metarhodopsin II occurred (see Figure 6). This

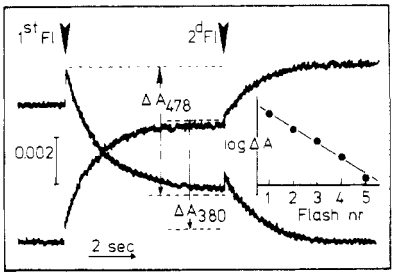

FIGURE 7: Kinetics of the metarhodopsin I to metarhodopsin II transition in filter paper disks. The RLCs in ether were prepared and layered (150 μL) on the disks as described under Materials and Methods. Disks were hydrated with 1:1 glycerol–66 mM phosphate buffer, pH 7.0, and cooled to 0 °C. Absorbance changes were recorded simultaneously at 478 and 380 nm, corresponding to the λ_{max} of metarhodopsin I and II, respectively. An upward deflection indicates an increase in absorbance (vertical scale). The arrowheads represent the time at which the flash was triggered. The inset shows the relation between the log of the absorbance change amplitude and the number of applied flashes. The $\tau_{1/2}$ for this reaction at 0 °C and pH 7.0 was 1.62 ± 0.3 s.

behavior illustrates again the similarities between the native and the model systems.

Metarhodopsin I to II Transition. Figure 7 illustrates a typical kinetic experiment of the RLC deposited in filter paper disks. Absorbance changes are recorded simultaneously at two wavelengths, 478 (upper curve) and 380 (lower curve) nm, corresponding to the λ_{max} of metarhodopsin I and II, respectively. Upon flash illumination, there is an initial absorbance increase at 480 nm (not time resolved) followed by a decay; correspondingly, there is an absorbance increase at 380 nm. A second flash induces the same absorbance changes but of smaller amplitude. As shown in the inset, the amplitude of the flash-induced absorbance changes becomes progressively smaller as the number of flashes applied increases. A linear relation is derived between the log of the absorbance change and the flash number. The initial transient increase in absorbance at 478 nm reflects the formation of metarhodopsin I from rhodopsin because the absorbance of metarhodopsin I at 478 nm is higher than that of rhodopsin (see Figure 4). The decay of metarhodopsin I is directly correlated with the formation of metarhodopsin II as in a simple substrate–product relation. When the kinetics of absorbance change at 478 nm

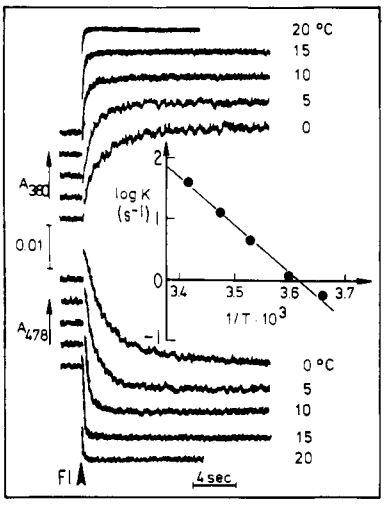

FIGURE 8: Arrhenius plot of the kinetics of the metarhodopsin I to metarhodopsin II transition in the filter paper disks. Disks prepared as described were hydrated with the usual buffer at pH 7.0. The actual experimental traces are all presented with the same time scale for the purpose of illustration. The points in the Arrhenius plot were obtained by expanding the traces appropriately and determining their $\tau_{1/2}$. The line was obtained from a least-squares fit of the data, and its correlation coefficient was 0.995.

is plotted vs. that at 380 nm, a straight line with slope at 45° is obtained. This confirms the kinetic correspondence of conversion between the two photointermediates.

Temperature and pH Dependences of the Metarhodopsin I to II Transition. The photoconversion kinetics of metarhodopsin I to metarhodopsin II were studied at five different temperatures in the range of 0–20 °C. The time courses of the absorbance changes at both 478 and 380 nm are illustrated in Figure 8. The corresponding rate constants, calculated as a first-order decay, are presented in the form of an Arrhenius plot in the inset of Figure 8. Our results indicate that the decay of metarhodopsin I consists of at least two first-order processes. For comparison of the rate of metarhodopsin I decay in different systems, the $\tau_{1/2}^{-1}$ value is used as a measure of rate. This criterion was shown by Baker et al. (1977) to be useful for a qualitative comparative analysis. The value of the activation energy derived from the temperature dependence of the reaction, 38.0 kcal/mol at pH 7.0, is in reasonable agreement with reported values obtained on sonicated ROS: 33.7 (Von Sengbusch & Stieve, 1971), 35 (Pratt et al., 1964; Applebury et al., 1974), and 34 (Hoffman et al., 1978) kcal/mol.

The fact that the decay is not a single first-order process is in agreement with results obtained by using sonicated ROS (Pratt et al., 1964; Applebury et al., 1974; Baker et al., 1977; Hoffmann et al., 1978), detergents (Applebury et al., 1974; Baker et al., 1977), and rhodopsin–phospholipid recombinants (Applebury et al., 1974). Analysis of several decay curves obtained at 0 °C and pH 7.0 as two independent first-order process gave a fast component ($\tau_{1/2} = 0.59 \pm 0.2$ s) amounting to 56 ± 14% of the amplitude and a slow one ($\tau_{1/2} = 3.5 \pm 1.65$ s) which contributes 44 ± 14% of the amplitude.

The metarhodopsin I to II photoconversion is a pH-dependent process (Matthews et al., 1963). Figure 9 illustrates traces of flash-induced decay of metarhodopsin I recorded at pH 5.5, 7.0, and 8.5. The reaction is faster at pH 5.5 and is progressively slower at more alkaline pH values. The lower portion of Figure 9 shows the corresponding exponential decay curves and the $\tau_{1/2}$ values: 0.53, 1.66, and 3.5 s at pH 5.5, 7.0, and 8.5 at 0 °C, respectively.

The bleaching sequence of rhodopsin is known to be arrested at the level of metarhodopsin I in anhydrous environments

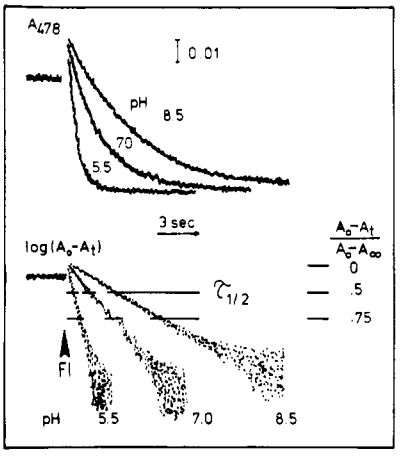

FIGURE 9: pH dependence of the metarhodopsin I decay in the filter paper disks. The disks prepared as described under Materials and Methods were hydrated with buffer at the indicated pH, and the experiment was performed at 0 °C. The lower half of the figure shows the exponential decay curves calculated from $\log A_0 - A_t$, where A_0 is the maximum absorbance at 478 nm and A_t is the absorbance at time t. The ratio $(A_0 - A_t)/(A_0 - A_\infty)$, where A_∞ denotes the absorbance at infinite time (eight lifetimes), represents the fraction of the total absorbance change which has occurred at the time t.

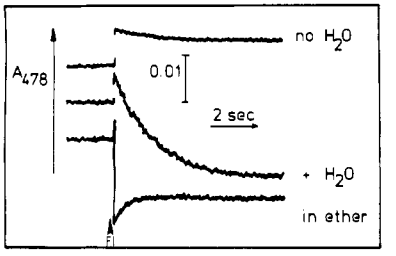

FIGURE 10: Metarhodopsin I decay in dry (upper curve) and hydrated filter paper disks (middle curve) and in ether (lower curve). Two disks were layered with RLC in ether (150 μL), as described under Materials and Methods. One of them was used dried, and the other was hydrated with 1:1 glycerol–phosphate buffer, pH 7.0. The lowest trace illustrates the metarhodopsin I decay in ether. The setup illustrated in Figure 1 was used, but the sample was in a spectrophotometer cuvette covered with a Teflon stopper and sandwiched between the two quartz rods (QR). All experiments were performed at 0 °C.

(Wald et al., 1950). The effect is reversible, and rhodopsin is completely bleached by introducing water into the system. As illustrated in Figure 10, the effect of water deprivation and subsequent hydration is also present in the model system of filter paper disks containing rhodopsin–lipid extracts. The upper record shows the lack of metarhodopsin I decay in the absence of water; the middle trace displays the typical conversion of metarhodopsin I to metarhodopsin II after the incorporation of water into the disks. The pH dependence of the reaction and the influence of hydration on the reaction rate confirm the notion that the kinetic competence of rhodopsin in the extracted form is preserved.

Metarhodopsin I to II Transition in Apolar Solvents. The results hitherto presented have described the properties of rhodopsin–lipid extracts deposited on filter paper disks after solvent removal. The photochemical activity of the extracted form of rhodopsin can also be demonstrated in the organic solvent. The kinetics of the flash-induced formation and decay of metarhodopsin I in hexane are similar to those obtained in the filter paper disks after ether evaporation or in ROS membranes (Applebury et al., 1974; Hoffman et al., 1978). In contrast, the process is drastically different in ether, as indicated in the lower curve of Figure 10: the formation and decay

of metarhodopsin I appear to proceed very fast and to be complete in less than 100 ms at 0 °C; this is followed by a slower recovery of absorbance at 478 nm.

The marked dependence of the reaction kinetics on the nature of the solvent establishes that the protein is sensitive to the environment. This observation taken together with the fact that rhodopsin is chemically regenerable in hexane but not in ether (Darszon et al., 1978a) suggests that bleached rhodopsin is susceptible to denaturation in ether but not in hexane.

Conclusions

The aim of this work is to establish the photochemical functionality of rhodopsin–lipid extracts in organic solvent and after solvent removal. The results indicate that rhodopsin–lipid complexes in hexane display the basic spectral features of rhodopsin as judged by the dark and bleached spectra, the capacity of opsin to regenerate, and the kinetics of the metarhodopsin I to II transition. Although the RLCs in ether appear to go through a different bleaching pathway and are not regenerable, when the solvent is evaporated in the dark and the residue studied in a filter paper, the rhodopsin spectral features are fully expressed, displaying a bleaching sequence similar to that of rhodopsin in retinal rod outer segments. This similarity is further substantiated by the kinetics and activation energy of the metarhodopsin I to II conversion in the filter paper as well as by the capacity of opsin to combine with 11-*cis*-retinal to regenerate rhodopsin. All of these criteria establish the spectral integrity of extracted rhodopsin. This crucial test of the adequacy of the manipulations required to reassemble biologically active rhodopsin-containing planar bilayers and other model membranes (Darszon et al., 1979; Montal, 1979) validates the notion that the reconstitution approach can lead to the understanding of the molecular physiology of signal transduction.

Acknowledgments

We are indebted to Professor Warren L. Butler for the generous availability of his spectrophotometric facilities, to Dr. W. E. Scott of Hoffmann-La Roche Laboratories for kindly supplying us with 11-*cis*-retinal, and to Eric Lighthart for his participation in the development of the data processing techniques.

References

Applebury, M. L., Zuckerman, D. M., Lamola, A. A., & Jovin, T. M. (1974) *Biochemistry 13*, 3448–3458.

Baker, B. N., Donovan, W. J., & Williams, T. P. (1977) *Vision Res. 17*, 1157–1162.

Butler, W. L., & Hopkins, D. W. (1970) *Photochem. Photobiol. 12*, 439–450.

Chien, T. F., & Mueller, P. (1976) *Fed. Proc., Fed. Am. Soc. Exp. Biol. 35*, 1599.

Darszon, A., Montal, M., & Philipp, M. (1977) *FEBS Lett. 74*, 135–138.

Darszon, A., Philipp, M., Zarco, J., & Montal, M. (1978a) *J. Membr. Biol. 43*, 71–90.

Darszon, A., Strasser, R. J., & Montal, M. (1978b) International Biophysics Congress (IUPAB), 6th, Kyoto, Japan, Abstr. VIII-12 (510), p 398.

Darszon, A., Vandenberg, C. A., Ellisman, M. H., & Montal, M. (1979) *J. Cell Biol. 81*, 446–452.

Ebrey, T. G. (1971) *Vision Res. 11*, 1007–1009.

Ebrey, T. G., & Honig, B. (1975) *Q. Rev. Biophys. 8*, 129–184.

Hagins, W. A. (1972) *Annu. Rev. Biophys. Bioeng. 1*, 131–158.

Hagins, W. A., & Yoshikami, S. (1977) in *Vertebrate Photoreception* (Barlow, H. S., & Fatt, P., Eds.) pp 97–139, Academic Press, New York.

Hecht, S., Schlaer, S., & Pirenne, M. H. (1942) *J. Gen. Physiol. 25*, 819–840.

Heller, J. (1968) *Biochemistry 7*, 2906–2913.

Hoffman, W., Siebert, F., Hofmann, K. P., & Kreutz, W. (1978) *Biochim. Biophys. Acta 503*, 450–461.

Hubbard, R., & Wald, G. (1952) *J. Gen. Physiol. 36*, 269–315.

Hubbell, W., Fung, F., Hong, K., & Chen, Y. S. (1977) in *Vertebrate Photoreception* (Barlow, H. S., & Fatt, P., Eds.) pp 41–59, Academic Press, New York.

Johnson, R. H., & Williams, T. P. (1970) *Vision Res. 10*, 85–93.

Kagawa, Y., & Racker, E. (1971) *J. Biol. Chem. 246*, 5477–5487.

Kawamura, S., Tokunaga, F., & Yoshizawa, T. (1977) *Vision Res. 17*, 991–999.

Matsumoto, H., Kasumi, H., & Yoshizawa, T. (1978) *Biochim. Biophys. Acta 501*, 257–268.

Matthews, R. G., Hubbard, R., Brown, P. K., & Wald, G. (1963) *J. Gen. Physiol. 47*, 215–240.

McConnell, D. G. (1965) *J. Cell Biol. 27*, 459–473.

Montal, M. (1974) in *Perspectives in Membrane Biology* (Estrada, S., & Gitler, C., Eds.) pp 591–622, Academic Press, New York.

Montal, M. (1979) *Biochim. Biophys. Acta 559*, 231–257.

Montal, M., & Korenbrot, J. I. (1973) *Nature (London) 246*, 219–221.

Montal, M., Darszon, A., & Trissl, H. W. (1977) *Nature (London) 267*, 221–225.

Montal, M., Darszon, A., & Strasser, R. J. (1978) in *Frontiers of Biological Energetics* (Dutton, P. L., Leigh, J. S., & Scarpa, A., Eds.) Vol. 2, pp 1109–1118, Academic Press, New York.

O'Brien, D. F., Costa, L. F., & Ott, R. A. (1977) *Biochemistry 16*, 1295–1303.

Ostroy, S. E. (1977) *Biochim. Biophys. Acta 463*, 91–125.

Papermaster, D. S., & Dreyer, W. J. (1974) *Biochemistry 13*, 2438–2444.

Paulsen, R., Miller, J. A., Brodie, A. E., & Bownds, D. (1975) *Vision Res. 15*, 1325–1332.

Pratt, D. C., Livingston, R., & Grellman, K. H. (1964) *Photochem. Photobiol. 3*, 121–127.

Shichi, H. (1971) *J. Biol. Chem. 246*, 6178–6182.

Strasser, R. J. (1973) *Arch. Int. Physiol. Biochim. 81*, 935–955.

Strasser, R. J., & Butler, W. L. (1976) *Biochim. Biophys. Acta 449*, 412–419.

Strasser, R. J., Darszon, A., & Montal, M. (1978) International Symposium on Visual Pigment and Purple Membrane, Kyoto University, Kyoto, Japan, p 26.

Tokunaga, F., Kawamura, S., & Yoshizawa, T. (1976) *Vision Res. 16*, 633–641.

Trissl, H. W., Darszon, A., & Montal, M. (1977) *Proc. Natl. Acad. Sci. U.S.A. 74*, 207–210.

Von Sengbusch, G., & Stieve, H. (1971) *Z. Naturforsch., B 26*, 488–489.

Wald, G. (1968) *Nature (London) 219*, 800–807.

Wald, G., & Brown, P. K. (1953) *J. Gen. Physiol. 37*, 189–200.
Wald, G., & Brown, P. K. (1956) *Nature (London) 177*, 174–176.
Wald, G., Durell, J., & St. George, R. C. (1950) *Science 111*, 179–181.
Yoshizawa, T. (1972) *Handb. Sens. Physiol. 7 (Part 1)*, 146–179.
Yoshizawa, T., & Wald, G. (1963) *Nature (London) 197*, 1279–1286.
Yoshizawa, T., & Wald, G. (1966) *Nature (London) 212*, 483–485.

Adsorption of Monovalent Cations to Bilayer Membranes Containing Negative Phospholipids†

Moisés Eisenberg, Thomas Gresalfi, Thomas Riccio, and Stuart McLaughlin*

ABSTRACT: The electrophoretic mobilities of multilamellar phosphatidylserine vesicles were measured in solutions containing monovalent cations, and the ζ potentials, the electrostatic potentials at the hydrodynamic plane of shear, were calculated from the Helmholtz–Smoluchowski equation. In the presence of 0.1 M lithium, sodium, ammonium, potassium, rubidium, cesium, tetraethylammonium, and tetramethylammonium chloride, the ζ potentials were −60, −62, −72, −73, −77, −80, −82, and −91 mV, respectively. Similar results were obtained with phosphatidylglycerol vesicles; different results were obtained with cardiolipin, phosphatidylinositol, and phosphatidic acid vesicles. The phosphatidylserine results are interpreted in terms of the Stern equation, a combination of the Gouy equation from the theory of the diffuse double layer, the Boltzmann relation, and the Langmuir adsorption isotherm. Evidence is presented that suggests the hydrodynamic plane of shear is 2 Å from the surface of the membrane in solutions containing the alkali metal cations. With this assumption, the intrinsic association constants of the above monovalent cations with phosphatidylserine are 0.8, 0.6, 0.17, 0.15, 0.08, 0.05, 0.03, and 0 M^{-1}, respectively. The validity of this approach was tested in two ways. First, the ζ potentials of vesicles formed from mixtures of phosphatidylserine and a zwitterionic lipid, phosphatidylcholine, were measured in solutions containing different concentrations of sodium. All the data could be described by the Stern equation if the "relaxation" of the ionic atmosphere, which is predicted by classic electrostatic and hydrodynamic theory to occur at low salt concentrations and high potentials, was circumvented by using only large (diameter >13 μm) vesicles for these measurements. Second, the fluorescent probe 2-(*p*-toluidinyl)naphthalene-6-sulfonate was used to estimate the potential at the surface of phosphatidylserine and phosphatidylglycerol vesicles sonicated in 0.1 M NaCl. Reasonable agreement with the predicted values of the surface potential was obtained.

This is the third paper in a series of reports on the interaction of inorganic cations with phospholipid bilayer membranes. Our ultimate objective is to understand how divalent cations such as calcium and magnesium interact with negative lipids commonly found in the bilayer component of biological membranes. As biological membranes contain zwitterionic as well as negative lipids, the interaction of cations with these lipids must also be investigated. It has been demonstrated that divalent cations adsorb to the zwitterionic lipid phosphatidylcholine (PC), that this adsorption can be described by the Stern equation (McLaughlin et al., 1978), and that calcium, but none of the other alkaline earth cations, adsorbs more strongly to PC bilayers in the gel than in the liquid-crystalline state (Lau et al., 1979). As biological solutions contain monovalent as well as divalent cations, we also need to know if ions such as sodium and potassium adsorb to a significant degree to negative lipids and if this adsorption can be described by the Stern equation. Phosphatidylserine (PS) is the predominant negative lipid in the membranes of many mammalian cells [e.g., White (1973)]; most of the experiments described below were performed on bilayers containing PS.

There is no completely satisfactory definition of specific adsorption. According to a "quasi-phenomenological" definition of Mohilner (1966) "one says there is specific adsorption if the experimental data cannot be explained by the theory of the diffuse double layer". In the absence of specific adsorption, the theory of the diffuse double layer [e.g., McLaughlin (1977)] predicts that all monovalent cations should exert identical effects on the surface potential of bilayer membranes containing negative lipids.

The first evidence for a specific interaction between the alkali metal cations and PS was obtained by Abramson et al. (1961). These authors noted that Na but not K, at concentrations of 0.4–0.7 M, produced a substantial coagulation of sonicated PS vesicles. Experiments by Hauser et al. (1975) demonstrated that both Na and K but not tetramethylammonium (TMA), at concentrations of 1 M, produced an increase in the optical density of a solution of sonicated PS vesicles. These experiments suggest that the interaction of these cations with PS decreases in the sequence Na > K > TMA. The first quantitative evidence that there was indeed a marked difference in the ability of a variety of monovalent cations to interact with PS was obtained by Puskin (1977). Using electron paramagnetic resonance measurements, he showed that divalent Mn ions were displaced from sonicated PS vesicles by monovalent cations. The relative association constants for Mn in decimolar solutions of Li, Na, K, Rb, Cs, and TMA were 0.31, 1.0, 1.1, 1.3, 1.4, and 7.1, respectively. This marked difference in the ability of Na and TMA to inhibit the binding of Mn to PS led Puskin to suggest that "(a) some specific Na–PS binding or (b) complications arising from penetration of cations into the restricted spaces between the

† From the Health Sciences Center, State University of New York at Stony Brook, Stony Brook, New York 11794. *Received April 17, 1979.* This work was supported by Grant GM 24971 from the U.S. Public Health Service and Grant PCM 79-03241 from the National Science Foundation.

0006-2960/79/0418-5213$01.00/0